

# Microscopy Cell Segmentation via Convolutional LSTM Networks

Assaf Arbelle, Tammy Riklin Raviv

Department of Electrical and Computer Engineering, Ben Gurion University

**Abstract.** Live cell microscopy sequences exhibit complex spatial structures and complicated temporal behaviour, making their analysis a challenging task. Considering cell segmentation problem, which plays a significant role in the analysis, the spatial properties of the data can be captured using Convolutional Neural Networks (CNNs). Recent approaches show promising segmentation results using convolutional encoder-decoders such as the U-Net. Nevertheless, these methods are limited by their inability to incorporate temporal information, that can facilitate segmentation of individual touching cells or of cells that are partially visible. In order to accommodate cell dynamics we propose a novel segmentation approach which integrates Convolutional Long Short Term Memory (C-LSTM) with the U-Net. The network’s unique architecture allows it to capture multi-scale, compact, spatio-temporal encoding in the C-LSTMs memory units. Promising results, surpassing the state-of-the-art, are presented. The code is freely available at: TBD

## 1 Introduction

Live cell microscopy imaging is a powerful tool and an important part of the biological research process. Nevertheless, the research is hindered by the exhaustive process of annotating the acquired sequences. These annotations are crucial for the quantitative analysis of properties such as cell size, mobility, and protein levels. Recent developments in the computer vision community have shown the strengths of Convolutional Neural Networks (CNNs) which surpass state-of-the-art methods in virtually all fields, such as object classification [10], detection [13], semantic segmentation [11], and many other tasks. Attempts at cell segmentation using CNNs include [3,9,14]. All these methods, however, are trained on independent, non sequential, frames and do not incorporate any temporal information. This can be a significant drawback in cases of neighboring cells that are hard to separate or when a cell partially vanishes. There are, however, non-deep learning methods that utilize the temporal information by combining tracking information from individual cells to support segmentation decisions [1,2,16,4].

A Recurrent Neural Network (RNN) is an artificial neural network equipped with feed-back connections. This unique architecture makes it suitable for the analysis of dynamic behavior. A special variant of RNNs is Long Short Term Memory (LSTM), which includes an internal memory state vector with gating

operations thus stabilizing the training process [7]. Common LSTM based applications include natural language processing (NLP) [19], audio processing [15] and image captioning [21].

Convolutional LSTMs (C-LSTMs) accommodate locally spatial information in image sequences by replacing matrix multiplication with convolutions [20]. The C-LSTM has recently been used to address the analysis of both temporal image sequences, such as next frame prediction [12], and volumetric data sets [5,17]. In [17] C-LSTM is applied in multiple directions for the segmentation of 3D data represented as a stack of 2D slices. Another approach for 3D segmentation is proposed in [5], where the output of a U-Net architecture is fed into bi-directional C-LSTMs.

In this paper we introduce the integration of C-LSTMs into an encoder-decoder structure (U-Net) allowing compact spatio-temporal representations in multiple scales. We note that, unlike [5], the proposed novel architecture is an intertwined composition of the two concepts rather than a pipeline. Our framework is assessed using time-lapse microscopy data where both cells' dynamics and their spatial properties should be considered. Specifically, we tested our method on the ISBI Cell Tracking Challenge: <http://www.celltrackingchallenge.net/latest-results.html>. Our method was ranked int the top three by the challenge organizers on the several submitted data set surpassing in some cases leading methods such as the U-Net [18].

The rest of the paper is organized as follows. Section 2 presents a probabilistic formulation of the problem and elaborates on the proposed network. Technical aspects are detailed in Section 3. In Section 4 we demonstrate the strength of our method, presenting state-of-the-art cell segmentation results. We conclude in Section 5.

## 2 Methods

We address individual cells' segmentation from microscopy sequences using C-LSTM. The main challenge in this type of problems is not only foreground-background classification but also the separation of adjacent cells. As in [3] we suggest to enhance individual cells' delineation by a partitioning of the image domain  $\Omega \in \mathbb{R}^2$  into three classes: foreground, background, and edges. We set  $C = \{0, 1, 2\}$  to denote these classes, respectively. Let  $\{I_t\}_{t=1}^T$  be the input image sequence, where  $I_t : \Omega \rightarrow \mathbb{R}$  is a grayscale image. We define a network  $f_\Theta$  with parameters  $\Theta$  as follows:

$$(o_t, h_t) = f_\Theta(I_t, o_{t-1}, h_{t-1}), \quad c \in C \quad (1)$$

where, the output  $o_t : \Omega \rightarrow \mathbb{R}^3$  is a three-dimensional feature vector corresponding to each input pixel  $\mathbf{x} \in \Omega$  and  $h_t$  are the hidden variables of the network. We define the pixel label probabilities using the softmax equation:

$$p(c|o_t(\mathbf{x})) = \frac{\exp\{[o_t(\mathbf{x})]_c\}}{\sum_{c' \in C} \exp\{[o_t(\mathbf{x})]_{c'}\}} \quad (2)$$

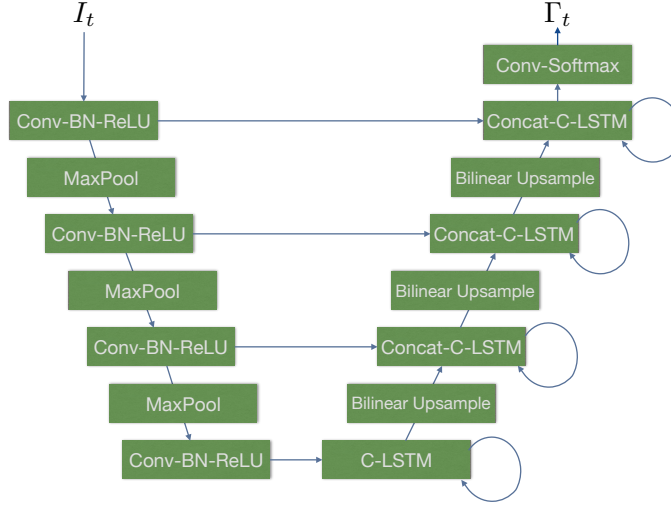


Fig. 1: The U-LSTM network architecture. The down-sampling path (left) consists of convolutional layers, followed by batch normalization and ReLU activations, the output is then down-sampled and passed to the next layer. The up-sampling path (right) consists of a concatenation of the input from the lower layer with the parallel layer from the down-sampling path followed by a C-LSTM layer and a bilinear up-sampling interpolation.

**Network Architecture** The proposed network  $f_{\theta}$  incorporates C-LSTM blocks into the U-Net architecture. While the U-Net [14] and C-LSTM [20] are widely used, their composition is suggested here for the first time and is shown to be powerful. The U-Net architecture, built as an encoder-decoder with skip connections, is able to extract meaningful descriptors at multiple image scales. However, this alone does not account for the cell specific history that can significantly support the segmentation. The introduction of C-LSTM blocks into the network’s decoder allows considering past cell appearances by holding their compact representations in the memory units. The network is fully convolutional and, therefore, can be used with any image size<sup>1</sup> during both training and testing. Figure 1 illustrates the full network architecture detailed in Section 3.

**Training** During the training phase the network is presented with a full sequence and manual annotations  $\{I_t, \Gamma_t\}_{t=1}^T$ , where  $\Gamma_t : \Omega \rightarrow [0, 1, 2]$  are the ground truth (GT) labels for the pixels in image  $I_t$ . The network is trained using Truncated Back Propagation Through Time (TBPTT). At each back propagation step the network is unrolled to  $\tau$  time-steps. The loss is defined using

<sup>1</sup> In order to avoid artefacts it is preferable to use image sizes which are multiples of eight due to the three max-pooling layers.

the cross-entropy loss:

$$L = \sum_{t'=t}^{t+\tau} \sum_{\mathbf{x} \in \Omega} p(\Gamma_{t'}(\mathbf{x}) | o_{t'}(\mathbf{x})) \quad (3)$$

and the weights are updated using gradient descent. Note that this loss differs from the U-Net loss, where boundary pixels are labelled as background weighted by their proximity to the two nearest cells [14]. Here, since a separate class for boundary pixels is defined, weighting is not required. Figure 2 show a visual example of the annotations and the network output. Comparisons of the two losses using the proposed network architecture is reported in the supplementary material.

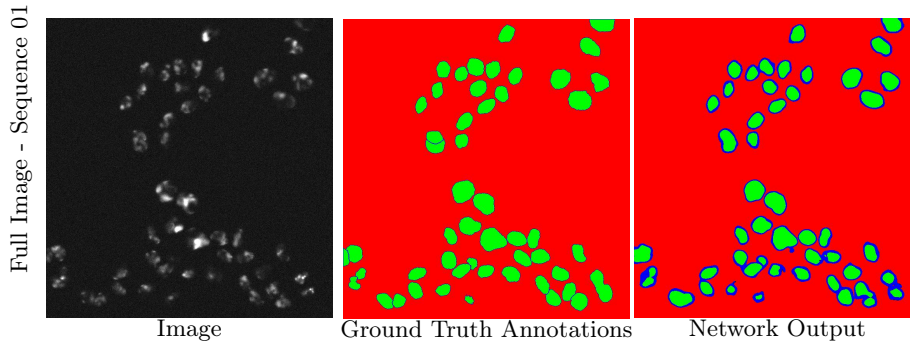


Fig. 2: Annotation Example: The visualization of the annotations as a three-class segmentations. On the left an image from the Fluo-N2DH-SIM+ data set, the center image is the GT annotation and the right image is the network output. The colors red, green and blue represent the three classes, background, foreground and cell contour, respectively. It is evident that the network learned to classify the contour of the cells as class edge allowing the separation of individual cells.

### 3 Implementation Details

**Architecture** The network comprises four down-sampling blocks and four up-sampling blocks. Each block in the down-sampling branch is composed of a convolutional layer, batch normalization [8], and leaky ReLU. The up-sampling blocks consist of a bilinear interpolation, a concatenation with the parallel down-sample block and a C-LSTM. All convolutional layers use kernel size  $3 \times 3$  with layer depths (32, 64, 128, 256). All maxpool layers use kernel size  $2 \times 2$  without overlap. All C-LSTM kernels are of size  $7 \times 7$  with layer depths (32, 64, 128, 256). The last convolutional layer uses kernel size  $1 \times 1$  with depth 3 followed by a softmax layer to produce the final probabilities (see Figure 1).

**Training Regime** We trained the networks for approximately  $100K$  iterations with an RMS-Prop optimizer [6] as implemented in Tensorflow (version 1.4.0) with learning rate of 0.0001. The unroll length parameter  $\tau$  was set to five (Section 2) and the batch size was set to three sequences.

**Data** The images were annotated using three labels for the background, cell nucleus and nucleus contour. The cell edge was defined as a single pixel wide contour of each cell nucleus. In order to increase the variability, the data was randomly augmented spatially and temporally by: 1) random horizontal and vertical flip, 2) random  $90^\circ$  rotation 3) random crop of size  $M \times M$  4) random sequence reverse  $([T, T - 1, \dots, 2, 1])$ , 5) random temporal down-sampling by a factor of  $k \in [0, 4]$ . The total training set following the proposed augmentation is hundreds of times larger than the original set. We note that the grayscale values are not augmented as they are biologically meaningful.

## 4 Experiments and Results

### 4.1 Evaluation Method

We evaluated the method using the scheme proposed in the online version of the Cell Tracking Challenge. Specifically, SEG for segmentation, as defined in [18]. The SEG measure is defined as the mean Jaccard index  $\frac{|A \cap B|}{|A \cup B|}$  of a pair of ground truth label  $A$  and its corresponding segmentation  $B$ . A segmentation is considered a match if  $|A \cap B| > \frac{1}{2}|A|$ .

**Challenge:** The method was applied to the five data sets from the ISBI Cell Tracking Challenge: Fluo-N2DH-SIM+, DIC-C2DL-HeLa, PhC-C2DL-PSC, Fluo-N2DH-GOWT1, Fluo-N2DL-HeLa. It is ranked 1st place in the SEG for the Fluo-N2DH-SIM+ data set measure surpassing state-of-the-art methods, such as U-Net (FR-Ro-GE) [14]. Table 2 reports our results in comparison to the three other leading methods provided by the challenge organizers. Visualizations of the results are presented in Fig 3. The quantitative results for all leading methods are publicly available at the ISBI Cell Tracking Challenge web sites: <http://www.celltrackingchallenge.net/latest-results.html>.

## 5 Summary

Time-lapse microscopy cell segmentation is, inherently, a spatio-temporal task. Human annotators frequently rely on temporal queues in order to accurately separate neighbouring cells and to detect partially visible cells. In this work, we demonstrate the strength of integrating temporal analysis, in the form of C-LSTMs, into a well established network architecture (U-Net). The resulting

---

<sup>2</sup> Due to anonymous submission, our results are presented as Anonymous Contributor.

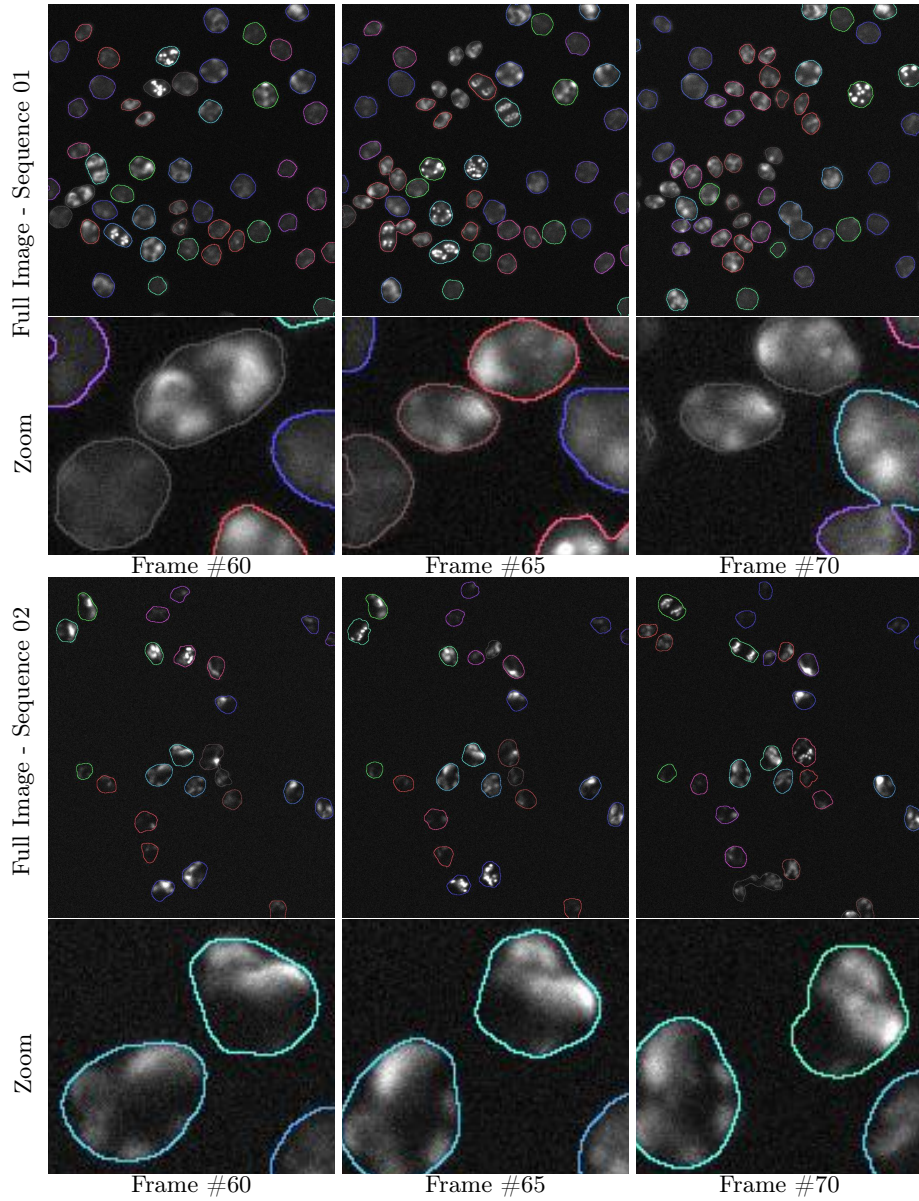


Fig. 3: Visual Results: An example for the segmentation of the test sequences at five frame intervals. The odd rows show the full image and the even rows show a zoom-in of a specific area. The top pair is part of the Fluo-N2DH-SIM+-01 sequence. Note that even though the cells are touching, the boundaries correctly separate them. The bottom pair is part of the Fluo-N2DH-SIM+-01 sequence. Note that the segmentation correctly includes invisible parts of the cells. This is thanks to the C-LSTM units which propagate information through time.

Dataset	Our Score (AC <sup>(1)2</sup> )	First	Second	Third
<b>Fluo-N2DH-SIM+</b>	<b>80.2%</b>	KTH-SE 79.2%	FR-Ro-GE 78.1%	PAST-FR 77%
<b>DIC-C2DL-HeLa</b>	51.2%	AC <sup>(2)</sup> 81.4%	FR-Ro-GE 77.6%	CVUT-CZ 46.4%
<b>PhC-C2DL-PSC</b>	61.1%	HD-Hau-GE 66.5%	CVUT-CZ 62.2%	KTH-SE 60.2%
<b>Fluo-N2DH-GOWT1</b>	85.4%	KTH-SE 92.7%	LEID-NL 89.3%	CUNI-CZ 88.7%
<b>Fluo-N2DL-HeLa</b>	83.9%	FR-Ro-GE 90.3%	KTH-SE 89.3%	CVUT-CZ 86.9%

Table 1: **Quantitative Results:** Method evaluation on three of the submitted dataset (challenge set) as published by the ISBI Cell Tracking Challenge organizers [18]. Our method ranked first, third and third in the Fluo-N2DH-SIM+, DIC-C2DL-HeLa, PhC-C2DL-PSC datasets, respectively. The columns three columns on the right report the results of the current top three methods as named by the challenge organizers. The SEG measure is explained in Section 4.1.

novel architecture is able to extract meaningful features at multiple scales and propagate them through time. This enables the network to accurately segment cells in difficult scenarios where the temporal queues are crucial. The method was tested on the five data set from the ISBI Cell Tracking Challenge. Quantitative analysis, presented in Section 4, shows that our method achieves state-of-the-art results. The code, implemented in Tensorflow, is freely available at: ANONYMOUS.

## References

1. Fernando Amat, William Lemon, Daniel P Mossing, Katie McDole, Yinan Wan, Kristin Branson, Eugene W Myers, and Philipp J Keller. Fast, accurate reconstruction of cell lineages from large-scale fluorescence microscopy data. *Nature methods*, 2014.
2. Assaf Arbelle, Nir Drayman, Mark Bray, Uri Alon, Anne Carpenter, and Tammy Riklin-Raviv. Analysis of high throughput microscopy videos: Catching up with cell dynamics. In *MICCAI 2015*, pages 218–225. Springer, 2015.
3. Assaf Arbelle and Tammy Riklin Raviv. Microscopy cell segmentation via adversarial neural networks. *arXiv preprint arXiv:1709.05860*, 2017.
4. Assaf Arbelle, Jose Reyes, Jia-Yun Chen, Galit Lahav, and Tammy Riklin Raviv. A probabilistic approach to joint cell tracking and segmentation in high-throughput microscopy videos. *Medical image analysis*, 2018.
5. Jianxu Chen, Lin Yang, Yizhe Zhang, Mark Alber, and Danny Z Chen. Combining fully convolutional and recurrent neural networks for 3d biomedical image segmentation. In *Advances in Neural Information Processing Systems*, pages 3036–3044, 2016.

6. Geoffrey Hinton. Rms prop: Coursera lectures slides, lecture 6.
7. Sepp Hochreiter and Jürgen Schmidhuber. Long short-term memory. *Neural computation*, 9(8):1735–1780, 1997.
8. Sergey Ioffe and Christian Szegedy. Batch normalization: Accelerating deep network training by reducing internal covariate shift. In *International conference on machine learning*, pages 448–456, 2015.
9. Oren Z Kraus, Jimmy Lei Ba, and Brendan J Frey. Classifying and segmenting microscopy images with deep multiple instance learning. *Bioinformatics*, 32(12):i52–i59, 2016.
10. Alex Krizhevsky, Ilya Sutskever, and Geoffrey E Hinton. Imagenet classification with deep convolutional neural networks. In *NIPS*, pages 1097–1105, 2012.
11. Jonathan Long, Evan Shelhamer, and Trevor Darrell. Fully convolutional networks for semantic segmentation. In *Proceedings of the IEEE CVPR*, pages 3431–3440, 2015.
12. William Lotter, Gabriel Kreiman, and David Cox. Deep predictive coding networks for video prediction and unsupervised learning. *arXiv preprint arXiv:1605.08104*, 2016.
13. Joseph Redmon, Santosh Divvala, Ross Girshick, and Ali Farhadi. You only look once: Unified, real-time object detection. In *Proceedings of CVPR*, pages 779–788, 2016.
14. Olaf Ronneberger, Philipp Fischer, and Thomas Brox. U-net: Convolutional networks for biomedical image segmentation. *arXiv preprint arXiv:1505.04597*, 2015.
15. Haşim Sak, Andrew Senior, and Françoise Beaufays. Long short-term memory recurrent neural network architectures for large scale acoustic modeling. In *Fifteenth annual conference of the international speech communication association*, 2014.
16. Martin Schiegg, Philipp Hanslovsky, Carsten Haubold, Ullrich Koethe, Lars Hufnagel, and Fred A Hamprecht. Graphical model for joint segmentation and tracking of multiple dividing cells. *Bioinformatics*, 31(6):948–956, 2014.
17. Marijn F Stollenga, Wonmin Byeon, Marcus Liwicki, and Juergen Schmidhuber. Parallel multi-dimensional lstm, with application to fast biomedical volumetric image segmentation. In *Advances in neural information processing systems*, pages 2998–3006, 2015.
18. Vladimír Ulman, Martin Maška, Klas EG Magnusson, Olaf Ronneberger, Carsten Haubold, Nathalie Harder, Pavel Matula, Petr Matula, David Svoboda, Miroslav Radojevic, et al. An objective comparison of cell-tracking algorithms. *Nature methods*, 14(12):1141, 2017.
19. Oriol Vinyals, Łukasz Kaiser, Terry Koo, Slav Petrov, Ilya Sutskever, and Geoffrey Hinton. Grammar as a foreign language. In *Advances in Neural Information Processing Systems*, pages 2773–2781, 2015.
20. Shi Xingjian, Zhourong Chen, Hao Wang, Dit-Yan Yeung, Wai-Kin Wong, and Wang-chun Woo. Convolutional lstm network: A machine learning approach for precipitation nowcasting. In *Advances in neural information processing systems*, pages 802–810, 2015.
21. Kelvin Xu, Jimmy Ba, Ryan Kiros, Kyunghyun Cho, Aaron Courville, Ruslan Salakhudinov, Rich Zemel, and Yoshua Bengio. Show, attend and tell: Neural image caption generation with visual attention. In *International Conference on Machine Learning*, pages 2048–2057, 2015.



## Appendix A

We examine the loss used in this paper, adopted from [3] compared with the loss originally proposed in [14]. In this paper we formulate the segmentation task using a three-class classification loss, for the background, foreground and cell contour. This intends to separate neighbouring cells with a thin line (of a single pixel width) and maximize the area of the true foreground segmentation. In [14], the same objective is approached using a two-class classification loss while increasing the weights of pixels which are near the border of two cells. In order to compare the the two losses we conducted the following experiment. The U-LSTM network, proposed here was trained twice with the same parameters, only changing the loss function. The Fluo-N2DH-SIM+ data set from the ISBI Cell Tracking Challenge was used as a training set due to it's full annotations. The validation was done on the Fluo-N2DH-GOWT1 data set from the "Training" set with publicly available annotations. Both networks were trained for 100K iterations. The results show a the advantage of the three-class loss, presented in Table 2.

Loss	Three-Class	Weighted Two-Class
Seq 01	<b>76.11%</b>	60%
Seq 02	<b>84.28%</b>	75.35%
Mean	<b>80.2%</b>	67.7%

Table 2: **Loss Comparison:** A comparison of the two loss functions: 1. Three-Class classification to foreground, background and edge as proposed by [3]. 2. Weighted Two-Class with increased weights for boundary pixels, as proposed by [14].